J Nanostruct 16(2): 2226-2233, Spring 2026

RESEARCH PAPER

Studying of the Antibacterial Properties of Ferric Ions Doped Zinc Oxide Nanoparticles

*Hasanain Salah Naeem [1] *, Sahar I. Naji [2], Israa Jaber [1], Bilal Majid Rudaini [3], Tammar Hussein Ali [1,4]*

[1] *College of Pharmacy, Al-Muthanna University, 66001 Samawah, Al Muthanna. Iraq*

[2] *Department of Pathological Analyses, College of Applied Medical Sciences, Al-Muthanna University, Al-Rumaytha 66002, Iraq*

[3] *Department of Pharmaceutical Chemistry, College of Pharmacy, University of Anbar, Ramadi, Iraq*

[4] *College of Pharmacy, National University of Science and Technology, 64001 Dhi Qar, Iraq*

ARTICLE INFO

Article History:
Received 07 January 2026
Accepted 26 March 2026
Published 01 April 2026

Keywords:
Antibiotic agent
Doped Nanoparticles
K. pneumoniae
MIC assay
S. aureus
Zinc oxide

ABSTRACT

Zinc oxide (ZnO) nanoparticles doped with 5% iron(III) exhibited enhanced antibacterial efficacy. Doped ZnO nanoparticles synthesized using co-precipitation, devoid of capping agents or surfactants, were characterized using X-ray diffraction (XRD), scanning electron microscopy (SEM), and energy dispersive X-ray spectroscopy (EDX). The results showed that the ZnO crystal lattice contains Fe(III) ions with a particle size ranging from 16 to 20 nm, and that ZnO has a wurtzite hexagonal structure. Nanoparticles of zinc oxide doped with iron showed detectable antibacterial action. Based on the findings of the minimum inhibitory concentration (MIC) tests, it was evident that the inhibitory impact of Fe(III)-doped ZnO nanoparticles was much stronger against Staphylococcus aureus (S. aureus) than Klebsiella pneumoniae (K. pneumoniae). Enhanced resistance is a result of the complex structure of gram-negative bacteria, particularly their outer membrane, which is thick with lipopolysaccharides and acts as a barrier to permeability. K. pneumoniae's distinctive polysaccharide capsule protects bacterial cells from antimicrobial agents and significantly increases the bacterium's virulence and resistance. Nanoparticles' size-constrained dispersion in solid media causes an underestimation of their actual antibacterial efficacy, in contrast to experiments conducted in liquids, which generally give a more accurate picture of their activity.

How to cite this article
Naeem H., Naji S., Jaber I., Rudaini B., Ali T . Studying of the Antibacterial Properties of Ferric Ions Doped Zinc Oxide Nanoparticles. J Nanostruct, 2026; 16(2):2226-2233. DOI: 10.22052/JNS.2026.02.067

INTRODUCTION

Nanoparticles (NPs) possess distinctive surface characteristics that render them optimal substitutes for existing materials and technologies in various lifestyle and biomedical applications. Recent studies in nanotechnology have recognized it as an effective instrument for numerous prevalent applications [1]. Due to the diverse range of pathogenic bacteria and their ability to acquire resistance, antibacterial medications are presently a big issue in the biomedical and healthcare industries. Here, a handful of NPs-dubbed "Nanoantibiotics"- have shown enhanced antibacterial action [2,3].

* *Corresponding Author Email: hasanain.salah@mu.edu.iq*

This work is licensed under the Creative Commons Attribution 4.0 International License.
To view a copy of this license, visit http://creativecommons.org/licenses/by/4.0/.

Zinc, iron, copper, and manganese are present in soil and cellular constituents in trace amounts. Consequently, the oxides of these metals are anticipated to offer superior biocompatibility at a reduced cost. Zinc oxide nanoparticles (ZnO NPs) are among the most extensively researched antibacterial agents due to their resistance to many antibiotics [4]. The Minimum Inhibitory Concentration (MIC) of ZnO nanoparticles is superior against many pathogenic strains when compared to other nanoparticles, including silver and copper oxide [5]. The primary antibacterial mechanism of these nanoparticles was the generation of Reactive Oxygen Species (ROS) and the induction of geno-toxicity. Reactive oxygen species (ROS) are unsuitable for medical applications as data indicates that even minimal amounts can harm human cells [6,7]. The antibacterial properties of ZnO have been demonstrated through (i) nanoscale reactive oxygen species (ROS) generation [8], (ii) the liberation of antibacterial Zn^{2+} ions [9], and (iii) direct engagement with the lipopolysaccharide of cell membranes [10], rendering it a more suitable nanoparticle in this context. Despite worries about its potential harm to human cells, zinc oxide has shown effective against specific types of superbugs [11].

Therefore, ZnO nanoparticles' potential medical uses are still under active research. It is imperative to lower the MIC values of ZnO Nano antibiotic and to establish a ROS-independent antibacterial mechanism for the effective therapeutic utilization of ZnO. Multiple research confirmed that the antibacterial efficacy of ZnO is contingent upon its size and morphology; hence, modifying the dimensions of ZnO crystals is anticipated to reduce MIC values [12,13]. Recent research from our group indicates that doping transition metal ions impacted the lattice properties, hence altering the mechanism and antibacterial activity of metal ion-based Nano antibiotics [14]. Rather than experiencing cell wall collapse, the bacterial cells were rendered inert. The antibacterial processes are influenced by the types and concentrations of dopants [15].

Furthermore, it is anticipated that metal ions with inherent antibacterial characteristics will synergistically augment the antibacterial efficacy of ZnO nanoparticles. An example is the enhanced antibacterial efficacy of iron-based compounds against diverse illnesses [16]. Iron-based nanoparticles exhibit a more rapid disintegration rate attributable to their magnetic characteristics, hence improving target efficiency for localized antibacterial activity [17]. Furthermore, Zn^{2+} possesses a larger ionic radius (0.074 nm) compared to Fe^{3+} (0.06 nm), suggesting it is likely to modify the structural defects of the ZnO lattice to improve its antibacterial efficacy without inducing cytotoxicity [18,19].

Consequently, we synthesized Fe(III) doped

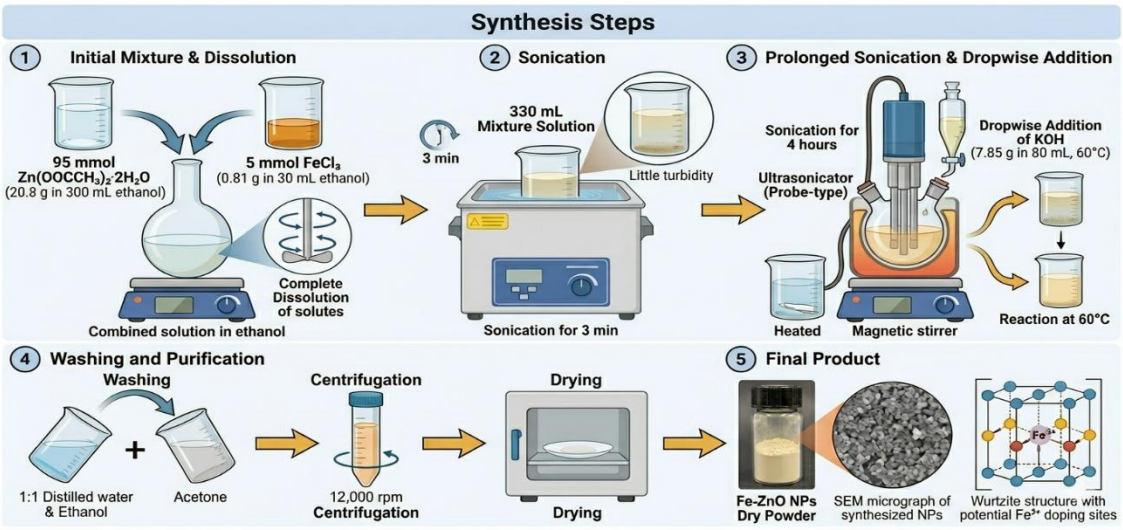

Fig. 1. Method for preparing the Fe-ZnO nanoparticles.

(cc) BY

ZnO nanoparticles (Fe-ZnO NPs) and examined their antibacterial efficacy and mode of action. The production of bimetallic Fe-ZnO nanoparticles was validated by various physical characterization techniques, including EDX and XRD. SEM was utilized to analyze the physical and chemical properties of Fe-ZnO, focusing on its morphology and structure. Two clinically relevant bacterial species, Gram positive (S. aureus) and Gram negative (K. pneumoniae), were tested to determine the antibacterial activity of the suggested nanoparticles. The MIC values were subsequently calculated. This study is beneficial for understanding the antibacterial activity of Fe-ZnO under standard settings.

MATERIALS AND METHODS

Materials and characterization

The primary materials utilised for the synthesis of Fe-ZnO nanoparticles were potassium hydroxide (KOH), ferric chloride ($FeCl_3$), and zinc acetate dihydrate ($C_4H_{10}O_6Zn$). Resazurin (7-Hydroxy-3H-phenoxazin-3-one 10-oxide) was among the fluorescent dyes employed to elucidate the antibacterial mechanism.

At ambient temperature, with parameters of 40 kV and 40 mA, employing Cu Kα radiation (d = 1.54 Å), the Bruker D8 X-ray diffraction AXS apparatus was used to acquire the XRD patterns of the nanoparticles. The surface morphology of the materials was investigated using an EI Quanta 400F SEM coupled with an Oxford-Instruments INCA 400 X-Max detector for EDX at 300 magnifications (spot size 1 mm x 1 mm) and an accelerating voltage of 20 kV.

Preparation of Fe-ZnO Nanoparticle

Iron(III)-doped zinc oxide nanoparticles (Fe-ZnO NPs) were produced via a co-precipitation method. 95 mmol (20.8 g in 300 mL) $Zn(OOCCH_3)_2.2H_2O$ and

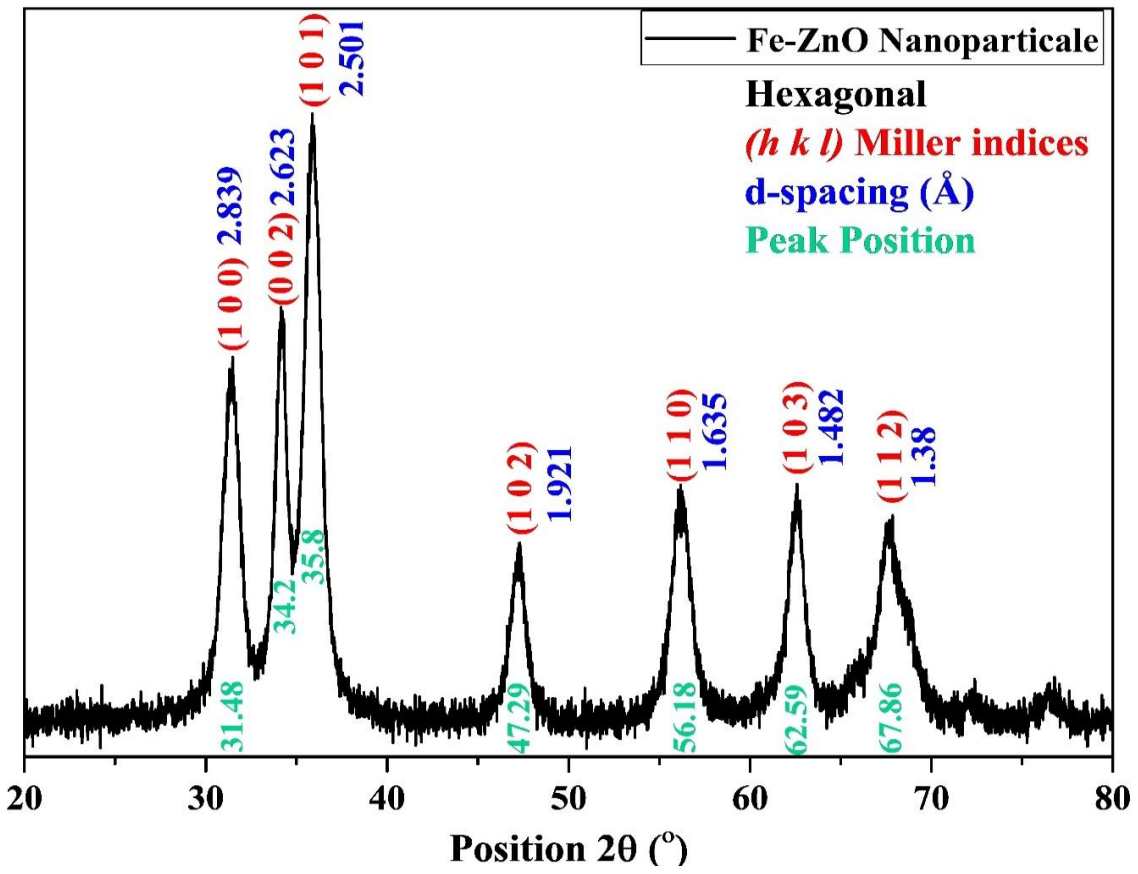

Fig. 2. XRD patterns of Fe-ZnO reflection patterns.

5 mmol (0.81 g in 30 mL) $FeCl_3$ were combined with ethanol and agitated thoroughly until complete dissolution of the solutes occurred. After that, 330mL of the mixture solution was subjected to sonication for 3 min. Following sonication, the solution exhibited little turbidity. The sonication process continued for 4 hours, with a gradual dropwise addition of (7.85g in 80mL) potassium hydroxide solution at 60°C, as shown in Fig. 1. The resultant dry powder was repeatedly washed with a 1:1 mixture of distilled water and ethanol, then with acetone, centrifuged at 12,000 rpm, dried, and stored.

Activity against bacteria

Minimum inhibitory concentration (MIC) determination

The Resazurin Microtitre-plate Assay (REMA) was modified to utilize a 96-well microtiter plate for assessing the MIC of Fe-ZnO nanoparticles against bacteria [20]. The adult male (35 years) wound infection was cultured for S. aureus. Urologists diagnosed an adult female (35 years) patient with a UTI after removing Klebsiella pneumoniae from her urine samples. Dispensed 100 µL of Mueller-Hinton broth (MHB) into each well of the microtiter plates under aseptic conditions. Subsequently, 100 µL of the test material was introduced into the first row of the 96-well plates. The test ingredient, Fe-ZnO NP, was serially diluted by transferring 100 µL from one well to another. The initial concentration of 50 mg/mL was reduced in successive halving increments (1/2, 1/4, 1/8, 1/16, 1/32, 1/64, and 1/128). Ten microlitres of bacterial solutions, each containing 1.5×10^8 CFU/ml of S. aureus and K. pneumoniae, were introduced into each well. The bacterial cultures were cultivated until they attained a 0.5 McFarland standard.

Subsequently, they were incubated at a temperature of 35±2°C for 18-24 hours after being loosely enveloped in Parafilm. The plate was re-incubated for a further 18-24 hours after incubation to observe any color change, after which 10 µl of resazurin solution (Alamar blue) was added to every well [21].

Agar diffusion assay

The antibacterial efficacy of the examined Fe-ZnO composites was evaluated utilizing the agar well diffusion technique. The first step was to mix 100 µl of freshly prepared Muller Hinton Agar (MHA) with 100 µl of 24-hour cultures of S. aureus and K. pneumoniae in BHI broth. The cultures were adjusted to a 0.5 McFarland standard during

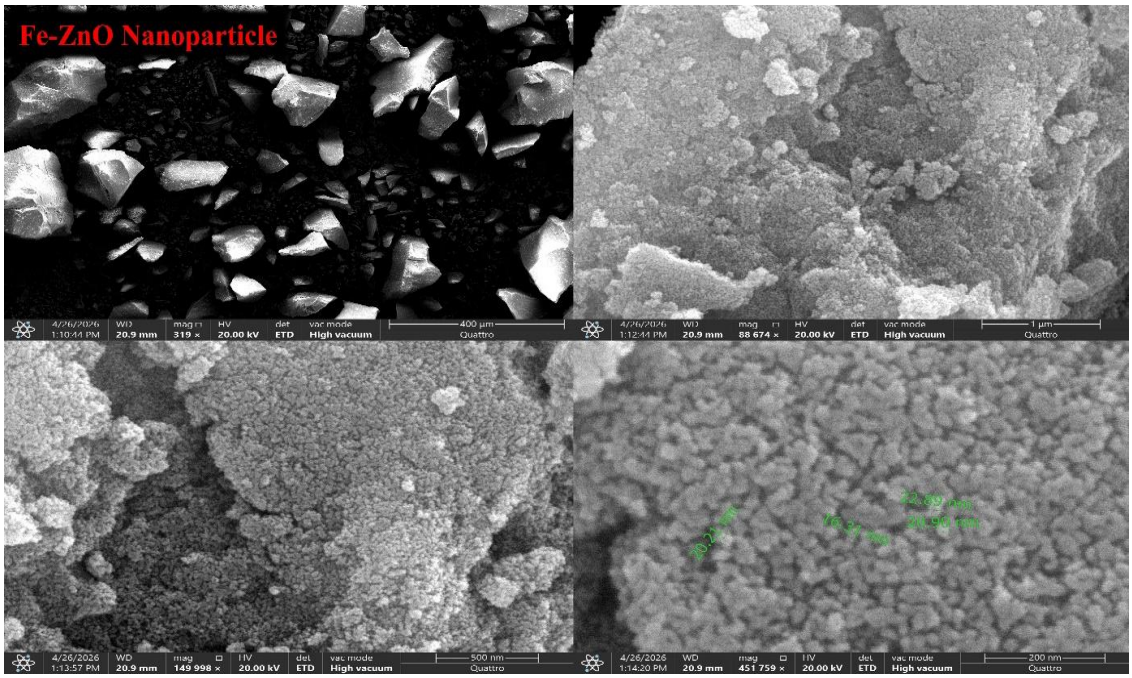

Fig. 3. SEM images of Fe-doped ZnO and SFEx@Fe-ZnO nanoparticles.

CC BY

the cooling phase (42 °C) after autoclaving. The amalgamation was subsequently placed onto Petri dishes. After the liquid solidified, a sterile cork borer was employed to form a single well (7 mm in diameter) in each plate. All tested Fe-ZnO compounds were subjected to the well, at MIC concentration. Following a 24-hour incubation of the plates at 37°C, the diameter of the inhibitory zone was determined in millimeters [22,23].

RESULTS AND DISCUSSION

Nanoparticle characterization

These ZnO nanoparticles with a 0.5% Fe(III) doping are shown in Fig. 2 in the XRD patterns. The Fe(III)-ZnO nanoparticle sample exhibits indexed diffraction peaks that indicate a hexagonal wurtzite structure belonging to the space group (P63mc). The diffraction data showed a high degree of agreement with the ZnO JCPDS card (JCPDS 36-1451). Doped Fe-ZnO samples did not show any evidence of pure Fe -or- Fe_2O_3 in their diffraction spectra. The efficient distribution of Fe(III) inside the ZnO lattice structure or the small amount of Fe(III) dopant used could be responsible for this [24].

Although undoped ZnO had narrower XRD peaks [25], Fe-ZnO exhibited wider peaks, indicating that crystallisation was hindered by Fe doping inside the ZnO lattice. Lattice instability and stress were both brought about by the addition of Fe(III) dopants to ZnO during crystallisation. Other research [26], has been shown that when smaller particles are combined with ZnO, they develop faster. This effect is caused by the fact that the ionic radii of Fe(III) ions are 0.067 nm and those of Zn(II) ions are 0.083 nm [27]. In XRD analysis, the lattice parameters of Fe-ZnO and ZnO were found to be a = b = 3.248 Å, c = 5.2054 Å and a = b = 3.249 Å, c = 5.206 Å, respectively, as previously reported [28]. The slightly lower lattice parameters of Fe-ZnO compared to ZnO demonstrated that the wurtzite structure could be preserved with the incorporation of Fe ions into the ZnO crystal lattice [29].

Scanning electron microscopy (SEM) produces high-resolution, pseudo-three-dimensional topography images of nanoparticles. Dimensions, form, surface morphology, and aggregation are critical structural characteristics that can be elucidated by scanning electron microscopy (SEM). Fig. 3 presents scanning electron micrographs of ZnO nanoparticles, either in their pure form or doped with iron. The micrographs indicate that the synthesized nanoparticles are aggregated and exhibit a spherical morphology. The doped ZnO displayed minor aggregation, while the photos

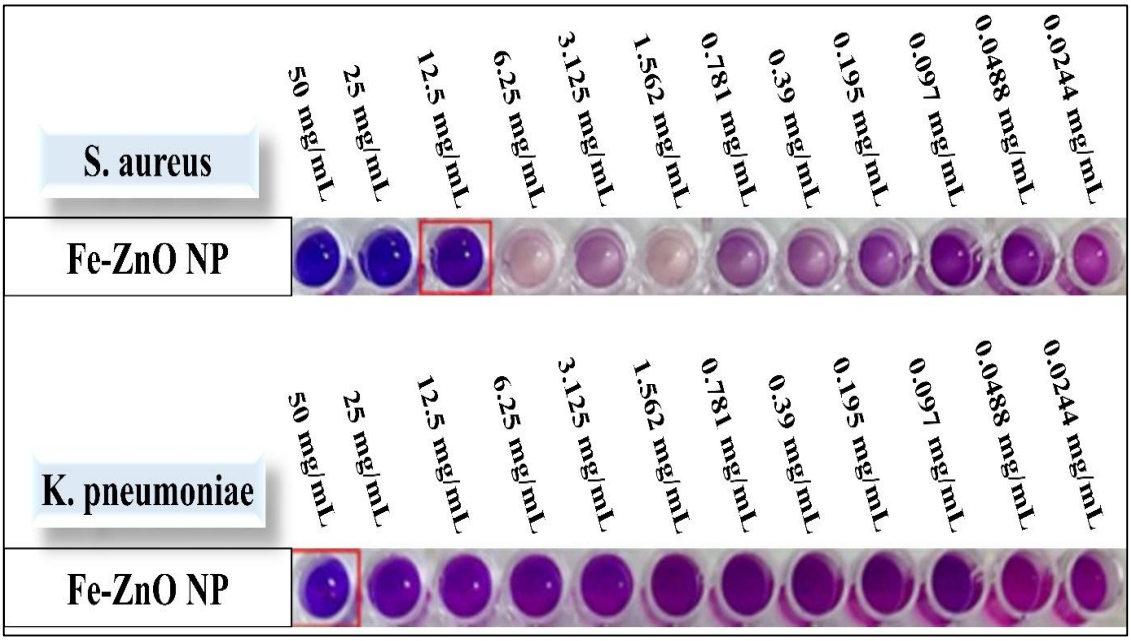

Fig. 4. EDS spectra of doped Fe-ZnO nanoparticle sample.

indicate that the Fe-ZnO particles predominantly assumed a spherical shape. Smaller Fe-ZnO particles are detected in samples with an increased number of Fe^{3+} ions [30]. The Fe-ZnO sample, exhibiting a particle size range of 16 to 20 nm, serves as a clear illustration of this phenomenon.

EDX was utilized to get a qualitative analyze of Fe-ZnO nanoparticles. This study elucidates the constituents present in the nanoparticle sample. Fig. 4 presents the results of the EDX study for the Fe-ZnO nanoparticle sample. Based on the EDX spectra, the synthetic Fe-ZnO sample contains primarily Zn and O, with very little Fe. The EDX spectral peak for O is observed at 0.5 keV, while Zn is detected at 1 keV, 8.6 keV, and 9.5 keV in the Fe-ZnO sample. The Fe signal manifests as diminutive

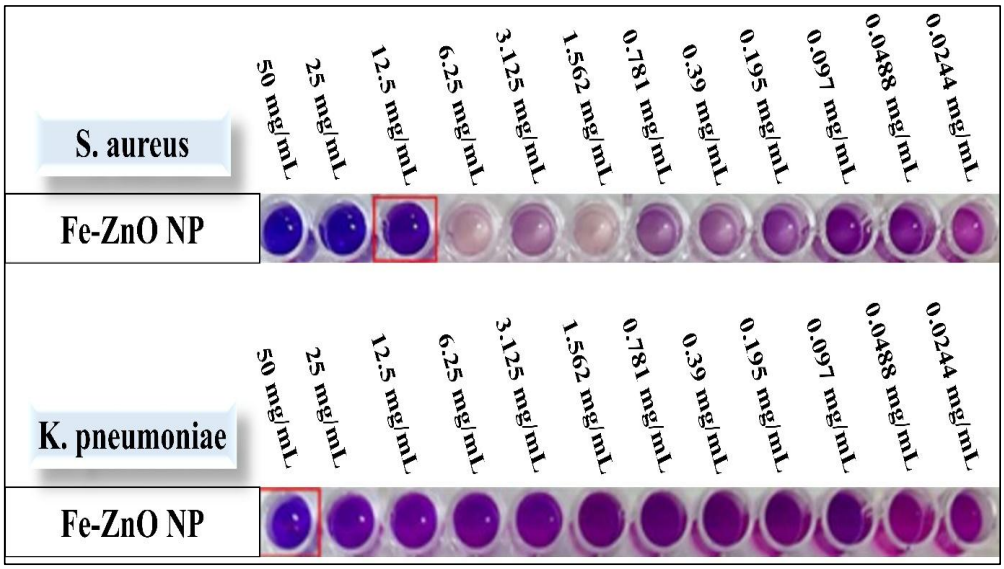

Fig. 5. MIC assay of Fe-ZnO nanoparticles against S. aureus and K. pneumonia.

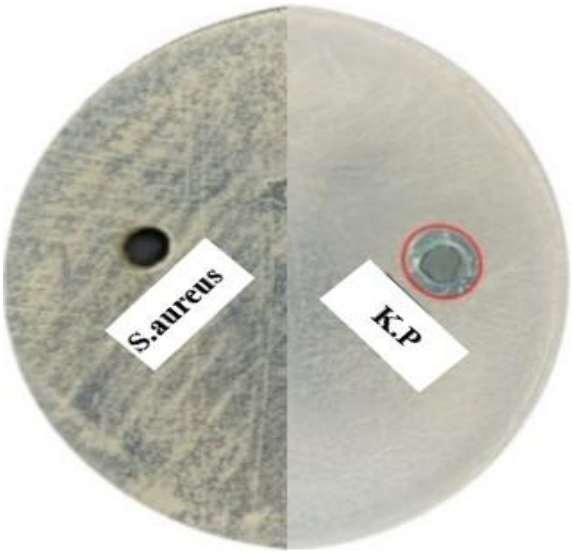

Fig. 6. Toxicity evaluation of Fe^{3+} doped ZnO nanoparticle degradation of S. aureus and K. pneumoniae using agar diffusion assay.

(cc) BY

peaks at 0.7 keV and 6.4 keV [31].

Particle Synthesis

Fe(III)-ZnO nanoparticles are synthesized by introducing a precipitating agent into a solution that contains dissolved zinc and iron precursors. The processes of metal hydroxide nucleation, growth, and calcination result in the development of a stable hexagonal wurtzite crystal structure with iron substitution. To prepare a homogeneous solution, dissolve the Zn^{2+} and Fe^{3+} ions in equal volumes of ethanol. The decomposition of the precursors into free metal ions in the solution yields solvated cations of Zn^{2+} and Fe^{3+}. A concentrated KOH solution is introduced dropwise while maintaining vigorous magnetic stirring. The introduction of OH^- ions to a solution results in a quick increase in pH. As seen in reactions 1 and 2, this results in the simultaneous precipitation of insoluble hydroxides, specifically 5% $Fe(OH)_3$ and 95% $Zn(OH)_2$.

$$Zn^{2+} + 2OH^- \rightarrow Zn(OH)_2 \quad (1)$$

$$Fe^{3+} + 3OH^- \rightarrow Fe(OH)_3 \quad (2)$$

Hydroxide undergoes fast nucleation when its concentration exceeds its solubility threshold. Due to the similarity between the ionic radius of Fe(III) (0.64 Å) and Zn(II) (0.83 Å) [27], the growing crystal lattice can accommodate Fe(III) ions instead of Zn(II) ions, leading to the creation of a framework doped with Fe(III).

Assessment of MIC Values

The effective was the synthesized nanoparticles against S. aureus and K. pneumoniae. We found out using the micro dilution method. The experiment started with a concentration of 50 mg/mL and was diluted twice. By observing the wells' consistent purple/blue coloration in Fig. 5, we were able to determine the MIC, which was found to prevent the development of identifiable bacteria. The third dilution showed the highest inhibitory action against S. aureus against Fe(III)-doped ZnO nanoparticles, with an estimated MIC value of 12.5 mg/mL. According to the MIC values for K. pneumoniae, Fe-ZnO nanoparticles demonstrated antibacterial efficacy at the initial dilution. This indicates a moderate inhibitory effect, with a MIC of around 50 mg / mL. According to the minimum inhibitory concentration (MIC) results, S. aureus exhibits greater susceptibility to Fe-ZnO nanoparticles than K. pneumoniae.

Agar diffusion assay

The antibacterial efficacy against S. aureus and K. pneumoniae was assessed utilizing the agar well diffusion technique with the synthesized Fe-ZnO nanoparticle, as shown in Fig. 6. The antibacterial efficacy of Fe(II)-doped ZnO nanoparticles against K. pneumoniae was demonstrated by the presence of distinct inhibition zones surrounding the wells. The lack of inhibitory zones for S. aureus indicates that Fe(II)-doped ZnO nanoparticles exhibited no measurable antibacterial activity under identical testing conditions. To determine how effective, the chemicals were against bacteria, we used the standard agar diffusion approach, which involves evaluating the presence and relative size of inhibition zones.

CONCLUSION

The co-precipitation method was employed to synthesize doped nanoparticles with mixed properties using zinc and ferric ions as dopants. Miniature Fe-ZnO nanoparticles, approximately 16 nm in size, were synthesized by gradually introducing a basic hydroxide solution into a solution containing selected transition metal ions. Characterization tests, including XRD, of Fe-ZnO samples have revealed a more prominent hexagonal wurtzite structure. Conversely, EDX analysis offered a comprehensive evaluation of the presence and quantities of each element in every sample. The detection of Fe(III) ions in Fe-ZnO particles signifies the successful execution of the process involving these nanoparticles, as recently disclosed. The results indicated that K. pneumoniae exhibited greater resistance to the majority of nanoparticle formulations than S. aureus, with MIC values of 50 mg/mL and 12.5 mg/mL, respectively.

ACKNOWLEDGMENT

The authors would like to express their gratitude to the Iraqi Ministry of Higher Education and Scientific Research, specifically the Faculty of Pharmacy at Al Muthanna University, for providing financial assistance for this paper.

CONFLICT OF INTEREST

The authors declare that there is no conflict of interests regarding the publication of this

CC BY

manuscript.

REFERENCE

1. Rezić I. Nanoparticles for Biomedical Application and Their Synthesis. Polymers. 2022;14(22):4961.
2. Shah KW, Huseien GF. Inorganic nanomaterials for fighting surface and airborne pathogens and viruses. Nano Express. 2020;1(3):032003.
3. Jiang J, Pi J, Cai J. The Advancing of Zinc Oxide Nanoparticles for Biomedical Applications. Bioinorg Chem Appl. 2018;2018:1-18.
4. Chinemerem Nwobodo D, Ugwu MC, Oliseloke Anie C, Al-Ouqaili MTS, Chinedu Ikem J, Victor Chigozie U, et al. Antibiotic resistance: The challenges and some emerging strategies for tackling a global menace. J Clin Lab Anal. 2022;36(9).
5. Asif N, Amir M, Fatma T. Recent advances in the synthesis, characterization and biomedical applications of zinc oxide nanoparticles. Bioprocess and Biosystems Engineering. 2023;46(10):1377-1398.
6. Lebaka VR, Ravi P, Reddy MC, Thummala C, Mandal TK. Zinc Oxide Nanoparticles in Modern Science and Technology: Multifunctional Roles in Healthcare, Environmental Remediation, and Industry. Nanomaterials. 2025;15(10):754.
7. Albukhaty S, Naderi-Manesh H, Tiraihi T, Sakhi Jabir M. Poly-l-lysine-coated superparamagnetic nanoparticles: a novel method for the transfection of pro-BDNF into neural stem cells. Artificial Cells, Nanomedicine, and Biotechnology. 2018;46(sup3):125-132.
8. Zhang B, Sun J-Y, Gao P-X. Low-Concentration NO_x Gas Analysis Using Single Bimodular ZnO Nanorod Sensor. ACS Sensors. 2021;6(8):2979-2987.
9. Wibowo A, Marsudi MA, Amal MI, Ananda MB, Stephanie R, Ardy H, et al. ZnO nanostructured materials for emerging solar cell applications. RSC Advances. 2020;10(70):42838-42859.
10. Noman MT, Amor N, Petru M. Synthesis and applications of ZnO nanostructures (ZONSs): a review. Crit Rev Solid State Mater Sci. 2021;47(2):99-141.
11. Comparison of Titanium Dioxide and Zinc Oxide Photocatalysts for the Inactivation of Escherichia coli in Water Using Slurry and Rotating-Disk Photocatalytic Reactors. American Chemical Society (ACS). http://dx.doi.org/10.1021/acs.iecr.3c00508.s001
12. Areeshi MY. A review on biological synthesis of ZnO nanostructures and its application in photocatalysis mediated dye degradation: An overview. Luminescence. 2023;38(7):1111-1122.
13. Yang L-Y, Dong S-Y, Sun J-H, Feng J-L, Wu Q-H, Sun S-P. Microwave-assisted preparation, characterization and photocatalytic properties of a dumbbell-shaped ZnO photocatalyst. J Hazard Mater. 2010;179(1-3):438-443.
14. Sirelkhatim A, Mahmud S, Seeni A, Kaus NHM, Ann LC, Bakhori SKM, et al. Review on Zinc Oxide Nanoparticles: Antibacterial Activity and Toxicity Mechanism. Nano-Micro Letters. 2015;7(3):219-242.
15. Ahmed N, Khalil Z, Farooq Z, Khizar ul H, Shahida S, Ramiza, et al. Structural, Optical, and Magnetic Properties of Pure and Ni–Fe-Codoped Zinc Oxide Nanoparticles Synthesized by a Sol–Gel Autocombustion Method. ACS Omega. 2023;9(1):137-145.
16. Lu J, Shi Z, Wang Y, Lin Y, Zhu Q, Tian Z, et al. Plasmon-enhanced Electrically Light-emitting from ZnO Nanorod Arrays/p-GaN Heterostructure Devices. Sci Rep. 2016;6(1).
17. Akram R, Almohaimeed ZM, Bashir A, Ikram M, Qadir KW, Zafar Q. Synthesis and characterization of pristine and strontium-doped zinc oxide nanoparticles for methyl green photo-degradation application. Nanotechnology. 2022;33(29):295702.
18. Wang ZL, Song J. Piezoelectric Nanogenerators Based on Zinc Oxide Nanowire Arrays. Science. 2006;312(5771):242-246.
19. Sutar SS, Patil SM, Kadam SJ, Kamat RK, Kim D-k, Dongale TD. Analysis and Prediction of Hydrothermally Synthesized ZnO-Based Dye-Sensitized Solar Cell Properties Using Statistical and Machine-Learning Techniques. ACS Omega. 2021;6(44):29982-29992.
20. Abdel-Salam M, Omran B, Whitehead K, Baek K-H. Superior Properties and Biomedical Applications of Microorganism-Derived Fluorescent Quantum Dots. Molecules. 2020;25(19):4486.
21. Sarker SD, Nahar L, Kumarasamy Y. Microtitre plate-based antibacterial assay incorporating resazurin as an indicator of cell growth, and its application in the in vitro antibacterial screening of phytochemicals. Methods. 2007;42(4):321-324.
22. Khalil M, Mohamed S, El-Naggar K. Green Synthesis of Silver Nanoparticles using Egyptian Propolis Extract and its Antimicrobial Activity. Egyptian Journal of Chemistry. 2021;0(0):0-0.
23. Balouiri M, Sadiki M, Ibnsouda SK. Methods for in vitro evaluating antimicrobial activity: A review. Journal of Pharmaceutical Analysis. 2016;6(2):71-79.
24. Liu H, Yang J, Zhang Y, Yang L, Wei M, Ding X. Structure and magnetic properties of Fe-doped ZnO prepared by the sol–gel method. J Phys: Condens Matter. 2009;21(14):145803.
25. Hammad TM, Griesing S, Wotocek M, Kuhn S, Hempelmann R, Hartmann U, et al. Optical and magnetic properties of Fe-doped ZnO nanoparticles prepared by the sol-gel method. International Journal of Nanoparticles. 2013;6(4):324.
26. Stojadinović S. Photocatalytic Degradation of Methyl Orange in Wastewater Using TiO_2-Based Coatings Prepared by Plasma Electrolytic Oxidation of Titanium: A Review. Reactions. 2025;6(2):25.
27. Das S, Sinha S, Das B, Jayabalan R, Suar M, Mishra A, et al. Disinfection of Multidrug Resistant Escherichia coli by Solar-Photocatalysis using Fe-doped ZnO Nanoparticles. Sci Rep. 2017;7(1).
28. Madkhali N. Analysis of Structural, Optical, and Magnetic Properties of (Fe,Co) Co-Doped ZnO Nanoparticles Synthesized under UV Light. Condensed Matter. 2022;7(4):63.
29. Imboon T, Sugio K, Khumphon J, Sridawong L, Mangala Gowri V, Yamada K, et al. Synergistic Effects of Fe-Doped ZnO and Graphene Oxide for Enhanced Photocatalytic Performance and Tunable Magnetic Properties. ACS Omega. 2025;10(31):34571-34587.
30. Djafarou R, Brahmia O, Benchikha N, Dokan FK, Sahmetlioglu E, Atoki AV, et al. Dual-Functional and Low-Toxicity ZnO Nanoparticles From Pomegranate Peel: Impact of Synthesis Parameters on Photocatalytic and Supercapacitive Performance. ChemistryOpen. 2026;15(5).
31. Anbuselvan D, Nilavazhagan S, Santhanam A, Chidhambaram N, Kanimozhi G, Ahamad T, et al. The effect of iron doping on the structural, optical, surface morphological, and temperature-dependent magnetic properties of ZnO nanoparticles. J Phys: Condens Matter. 2020;33(9):094001.

CC BY